

On the Evolution of Neuron Communities in a Deep Learning Architecture*

Sakib Mostafa¹ and Debajyoti Mondal¹

¹Department of Computer Science, University of Saskatchewan, Saskatoon, Canada,
sakib.mostafa@usask.ca, dmondal@cs.usask.ca

October 12, 2021

Abstract

Deep learning techniques are increasingly being adopted for classification tasks over the past decade, yet explaining how deep learning architectures can achieve state-of-the-art performance is still an elusive goal. While all the training information is embedded deeply in a trained model, we still do not understand much about its performance by only analyzing the model. This paper examines the neuron activation patterns of deep learning-based classification models and explores whether the models' performances can be explained through neurons' activation behavior. We propose two approaches: one that models neurons' activation behavior as a graph and examines whether the neurons form meaningful communities, and the other examines the predictability of neurons' behavior using entropy. Our comprehensive experimental study reveals that both the community quality (modularity) and entropy are closely related to the deep learning models' performances, thus paves a novel way of explaining deep learning models directly from the neurons' activation pattern.

1 Introduction

Deep learning allows the researchers to engineer better features and representation of data through representation learning [26]. Despite the widespread usage of deep learning methods, it is still considered a black box, and there is a lack of understanding of the working procedure of the models [36, 34, 45, 37]. Researchers often rely on intuition and domain knowledge when designing deep learning architectures [38]. They use the models' accuracy and loss to evaluate the performance and tune the hyperparameters to optimize the models [14, 15]. However, to gain a deeper insight into the model, it is crucial to look beyond its accuracy and loss, i.e., we need to design additional evaluation matrices that can provide a level of confidence in the model predictions and help understand the mechanism of the prediction.

Exploring network architecture helps explain why some models perform better than others. For example, by comparing the weight optimization against model architecture, Gaier and Ha [13] showed that a model's performance depends mostly on its architecture. Zhang et al. [50] created an explanatory graph that can disentangle different part patterns from feature maps of the convolutional neural network (CNN). Visual analytics tools have also been used to understand the architectures better. Hohman et al. [20] developed SUMMIT, a tool to visualize the features that the deep learning model is learning and understand the interaction between the features to make predictions. The authors used attribution graphs to analyze the neuron associations and substructures that affect the model's outcome. Gigante et al. [15] analyzed a neural network's performance using a visualization technique called Multislice PHATE, which uses multidimensional scaling to embed the diffusion geometry of a dataset in multiple dimensions. However, it is difficult to use Multislice PHATE without domain knowledge, and it does not provide quantitative measures for the evaluation.

*This work is supported by the Natural Sciences and Engineering Research Council of Canada (NSERC), and by two Canada First Research Excellence Fund (CFREF) grants coordinated by Global Institute for Food Security (GIFS) and Global Institute for Water Security (GIWS).

1.1 Motivation

In this paper, our main focus is on classification models. A deep learning model that performs a classification task is optimized to minimize the difference between the model’s prediction and the actual value. The prediction is recorded as accurate if it is above a threshold, and this process does not fully leverage the information hidden inside the architecture. The neuron activation pattern that appears during the training contains rich information that, if understood well, can potentially be combined with model prediction to provide a level of confidence in the prediction value. It may also allow us to design more efficient models and additional evaluation metrics to help reduce the number of false negatives and false positives. If it is possible to predict the model’s performance using the neuron activation pattern, we can understand when some models perform better than others by analyzing the pattern. This motivated us to explore different ways to examine neurons’ activation pattern and establish their relation to the training accuracy.

1.2 Contribution

We study the neuron activation pattern using two approaches: one based on a graph-theoretic model, and the other is based on an information-theoretic model. Our proposed metrics show a correlation with the training accuracy on both benchmark and real-life datasets in both cases.

- For the graph-theoretic approach, we created a novel ‘activation pattern graph’ model and showed that the set of neurons that are frequently and highly activated for a class often forms a community (i.e., an induced subgraph that contains more edges within than outside of the subgraph) in the activation pattern graph. We observed that modularity, a widely used metric to measure community quality, is closely related to the model’s training accuracy.
- For the information-theoretic model, we propose a novel method that allows us to measure the predictability of the neurons’ activation behavior leveraging entropy [16]. Our experimental results show that the entropy of the neurons is relevant to the model’s training accuracy.

2 Related Work

Shortliffe and Buchanan [41] were among the first researchers to describe the necessity of explaining the decisions made by expert systems. The expert systems have come a long way since then, but the explainability problem prevails as we build more complex artifacts such as deep learning models. There have been several attempts to explain deep learning models, which we review in this section.

2.1 Neuron Activation Pattern

Researchers have investigated both neuron activation patterns and loss function to explain deep learning models. Olah et al. [35] studied what the neurons respond to and proposed that neurons work in a group. Li et al. [28] showed a relationship between the performance of the deep learning model and the convexity of the loss function. Mahendran and Vedaldi [29] studied the feature maps of the CNN models to understand the activation pattern by inverting the models and showed that there is indeed a relation between the performance of the model and the activation pattern. Kim et al. [24] vectorized the activation values of hidden layers and created striped patterns to find relevance between pattern and decision. However, they experimented with a small dataset without directions for generalizability.

Bau et al. [2] studied the relation between the activation pattern and semantic concepts. They optimized the hyperparameters of the deep learning models and quantitatively analyzed the effect of changing different parameters. The relevance between activation patterns and semantic concepts was further studied by [11]. They created vector response of semantic concepts based on activation pattern and established that the neurons work in a group, and the same neuron can represent multiple concepts. We found a similar characteristic of the neuron activation pattern in our study, where there was an overlap of neurons representing multiple classes. However, with training, a class was represented by more unique neurons.

Another way of interpreting the deep learning models’ learning is by selecting image patches that maximize the neuron activation [48]. Zhou et al. [51] described scenes using the units from the feature

maps and also proposed that individual units behave as object detectors. Simon et al. [42] analyzed the deep learning model’s feature maps and found a spatial relation between the activation centers and the semantic parts or bounding boxes of the ground truth images. Zhang et al. [50] used hierarchical explanatory graphs across layers to propose a way of maximizing a deep learning model’s performance. Although there have been several attempts to explain activation patterns, in this paper we take a very different approach to the explanation of the neural network models by combining the graph-theoretic and information-theoretic approaches, which allow us to relate various quantitative measures to the model’s performance.

2.2 Visualization and Interpretability

Visualization is considered to be a promising approach for explaining complex systems, and as a result, there have been several attempts to explain the deep learning models using visualization tools [19, 6]. A dataflow diagram is a simple way to visualize a deep learning model’s architecture [46]. However, dataflow diagrams do not tell much about the model’s learning process.

Smikov et al. [44] proposed “Tensorflow Playground,” where users can train a model by changing the hyperparameters and observe the training process with various plots and charts. Harley [18], proposed an interactive visual inspection tool, where a model was trained on the MNIST dataset [27], and for input data, the tool showed which feature maps were activated and also which part of the input data was activating the maps. ACTIVIS [22] is an interactive visualization tool that, along with the dataflow diagram, provides a projection of the neuron activation for different instances. This only allows users to explore the activation pattern for different samples, classes, and subsets rather than explaining the model’s working procedure. CNNComparator [49] is a tool to compare the performance matrices and the distribution of hyperparameters of two deep learning models.

A rich body of research examines ways of visualizing feature maps of CNN models [9, 43, 48]. Such works focus mostly on features that are being learned from the feature maps and do not attempt to relate the learning process to model performances. The common limitation of most studies that rely on visualization is that the visual assessment is subjective and often hard to evaluate quantitatively or to relate with the model’s performance.

3 Technical Background

3.1 Graph and Community Structure

A *graph* consists of a set of elements (nodes) and a set of pairs of elements (edges), where the nodes represent objects and edges represent pairwise relationships. A *community* of a graph is defined as a subgraph that contains more edges within than the edges connecting them to the rest of the graph. Community detection algorithms often define a quality measure for the communities and then attempts to find a partition of the nodes that maximizes the quality measure [12, 32]. Later, we will define graphs with nodes as neurons and edges as their simultaneous activation. We will examine the communities of these graphs based on several quality measures as explained in the next section.

3.2 Modularity

Modularity is a widely used metric to assess the quality of a given set of non-overlapping communities [31, 10, 7]. The idea of modularity is based on comparing the given graph G with a random graph. Given two communities C_i and C_j in G , we use the notation $e(C_i, C_j)$ to denote the number of edges between these two communities. Let a_{C_i} be the fraction of all the edges connecting the community C_i to all other communities, i.e., $a_{C_i} = \sum_j e_{C_i C_j}$. For a random graph, the fraction of the resulting edges that connect nodes within the community C_i is $a_{C_i}^2$. Hence the modularity can be formalized as follows [32]:

$$Q_{no-overlap} = \sum_i (e_{C_i C_i} - a_{C_i}^2). \quad (1)$$

The minimum modularity value is 0, which represents the randomness of the graph, and a larger modularity score indicates better quality for the communities. Let A_{vw} be the adjacency matrix of G , and let m be

the number of edges in G . For a vertex v (resp., w) in G , we denote its degree and community by k_v and C_v (resp., k_w and C_w). Now, Eq. 1 can be written as follows [3]:

$$Q_{no-overlap} = \frac{1}{2m} \sum_{v,w} (A_{vw} - \frac{k_v k_w}{2m}) \delta(C_v, C_w), \quad (2)$$

$$\text{where } \delta(C_v, C_w) = \begin{cases} 1, & \text{if } C_v = C_w \\ 0, & \text{otherwise.} \end{cases}$$

In Eq. 2, $\frac{k_v k_w}{2m}$ represents the probability that two nodes v and w are connected in a random graph, and A_{vw} is 1 or 0 depending on whether v and w are adjacent in G or not. The term $\frac{1}{2m}$ is for normalizing the modularity value, and $\delta(C_v, C_w)$ regulates the algorithm only to consider the edges of a specific community.

The modularity above is defined only on a partition, i.e., when the communities are disjoint. Shen et al. [40] proposed an extension of Eq. 2 for undirected, unweighted graphs with overlapping communities, as follows:

$$Q_{unweighted,overlap} = \frac{1}{2m} \sum_{v,w} (A_{vw} - \frac{k_v k_w}{2m}) \frac{1}{O_v O_w}, \quad (3)$$

where O_v and O_w is the number of communities containing node v and w , respectively. Thus the modularity becomes larger when the communities have less overlap. Chen et al. [5] proposed a further extension for weighted, undirected graphs with overlapping communities, as follows:

$$Q_{weighted,overlap} = \frac{1}{2m} \sum_{c \in C} \sum_{v,w} (A_{vw} - \frac{k_v k_w}{2m}) \alpha_{cv} \alpha_{cw}, \quad (4)$$

where α_{cv} is the belonging coefficient [33] for a community c and vertex v is defined as follows:

$$\alpha_{cv} = \frac{k_{cv}}{\sum_{c \in C} k_{cv}} \text{ and } k_{cv} = \sum_{p \in c} W_{vp}.$$

where C is the set of community in graph G and $c \in C$, W_{vp} is the weight of the edge between node v and p . In Eq. 4, if node v belongs to only one community c , α_{cv} is equal to 1; if node v does not belong to community c , α_{cv} is equal to 0, which ensures the consistency of Eq. 4 with Eq. 2. Compared to Eq. 2, Eq. 4 considers overlapping communities similar to Eq. 3, but unlike Eq. 2 it considers the edge weights too. The benefit of Eq. 4 over other equations is, a pair of nodes within a community with higher edge weight contributes more to the quality measure compared to the pairs with low edge weight.

3.3 Entropy

Entropy is a metric that measures the level of uncertainty in a system, and a rich body of research examines different ways of measuring entropy [4]. Shanon entropy is a widely used metric in information theory [39], which calculates the average information available based on the probability of a variable's possible outcomes. Let X be a discrete random variable with possible outcomes x_1, x_2, \dots, x_k which occurs with probabilities $P(x_1), P(x_2), \dots, P(x_k)$, then the Shanon entropy, H of the variable X is defined as follows:

$$H = - \sum_{i=1}^k P(x_i) \log P(x_i). \quad (5)$$

A higher value of Shanon's entropy indicates a more uncertain outcome, which is more difficult to predict.

4 Hypothesis

We assume that if a neuron is frequently activated with a high activation value for a particular class, then the neuron is a representative of that class. Consider a graph with nodes as neurons and edges representing simultaneous activation of pairs of neurons. We refer to such a graph as an 'activation pattern graph', and describe the details in Section 5.1. Although one neuron can be representative for

multiple classes, over the training, we expect the class representatives to have less overlap. Hence we also expect the activation pattern graph to evolve such that the neurons representing a class form a community. Furthermore, over the training, the neurons are expected to have more certainty in their activation pattern for various classes (rather than being random). Therefore, we expect the ‘activation pattern entropy’, a measure related to the predictability of a neuron behavior, as described later in Section 5.2, to decrease. In particular, we examine the following hypotheses.

H1: The neurons that are frequently activated together form a community in the activation pattern graph.

H2: The modularity of the activation pattern graph is related to a deep learning model’s training performance.

H3: The entropy of the activation pattern is related to a deep learning model’s training performance.

5 Methodology

In this section, we describe the activation pattern graph and activation pattern entropy, which are at the core of our methodology and experimental design.

5.1 Activation Pattern Graph

Assume that there are C classes in the training dataset, and let D_i , where $1 \leq i \leq k$, be the subset corresponding to the i th class. Let ℓ be a fully connected layer in the neural network with n neurons. By the notation $v_i(q, \ell, d)$, we denote the activation value of a neuron $q \in \ell$ for a data d that belongs to the i th class. Thus the average activation value of a neuron q in layer ℓ for a class i is as follows:

$$V_i(q, \ell) = \frac{\sum_{d \in D_i} v_i(q, \ell, d)}{|D_i|}. \quad (6)$$

We construct the *activation pattern graph* G of a layer ℓ as follows. We first calculate each neuron’s average activation value for a class. Next, for every class, we select S neurons with the highest average activation value and take their union to create the vertex set of G . Let p, q be a pair of neurons in S and let $\delta_{p,q}$ be the number of data elements in D_i , where both p and q obtain activation values that are larger than their individual average activation values, i.e., $\delta_{p,q} = |\{d : d \in D_i, v_i(p, \ell, d) > V_i(p, \ell) \text{ and } v_i(q, \ell, d) > V_i(q, \ell)\}|$. Then, for class i , we create an adjacency matrix, $A_{i,\ell} = (a_{p,q})_{n \times n}$, where

$$a_{p,q} = \begin{cases} \frac{\delta_{p,q}}{|D_i|}, & \text{if } p \in S \text{ and } q \in S \\ 0, & \text{otherwise.} \end{cases} \quad (7)$$

The final adjacency matrix, A_ℓ of the activation pattern graph is computed as $A_\ell = \sum_{i=1}^k A_{i,\ell}$. Thus intuitively, an activation pattern graph maintains a set of neurons that are frequently activated, where a weighted edge between a pair of neurons represents the frequency of their simultaneous activation. We created a graph for every iteration and every fully connected layer (except the output layer).

5.2 Entropy of Activation Pattern

In a neural network with fully connected layers and ReLU (Rectified Linear Unit) as the activation function, the activation of each neuron is calculated as $ReLU(\mathbf{y}) = \max(0, \mathbf{y})$, where \mathbf{y} is the output of a layer. Let W_ℓ and \mathbf{B}_ℓ be the weight and bias of layer ℓ of a neural network. Then for an input I , the output of the layer ℓ is calculated as $\mathbf{y}_\ell = (W_\ell \times I) + \mathbf{B}_\ell$.

At the beginning of training, the weights and biases are randomly initialized, and over the training, these values are updated for improved predictions. The neuron activation thus gets more and more influenced by the classes present in the data. Due to random initial weights, the activation of the neurons also becomes unpredictable. In such a case, the activation patterns’ entropy is high, reflecting the system’s randomness. As the training progresses, the activation pattern is biased by the data, and thus the entropy will decrease.

We now compute the *activation pattern entropy* of a particular neuron, which is based on the idea of measuring the predictability of its activation value. We create a $|D| \times N$ activation pattern matrix, F , where $|D|$ is the size of the training dataset, and N is the total number of neurons in the architecture, except for the neurons in the last layer (output layer). Each entry (i, j) of F contains the activation value of the j th neuron subject to the i th element of the dataset D . We then compute a normalized matrix F_{norm} by dividing each column by the column sum, i.e., $F_{norm}(i, j) = \frac{F(i, j)}{\sum_{i=1}^{|D|} F(i, j)}$.

To examine the predictability of the activation value for j th neuron, we categorized its normalized activation values using R equal size bins. In other words, we create a histogram for the j th column values of $F_{norm}(i, j)$. The intuition is that if the neuron’s activation is unpredictable, then the histogram will not have well-defined maxima or contain many local maxima. Otherwise, it will be activated for one or only a few classes and likely to produce a global peak. There is an exception, where a neuron may never be activated and will create a global maxima at the bin that contains the 0 value. Therefore, to create the histogram, we only consider the non-zero activation values. Let B_k and H_k , where $1 \leq k \leq R$, be the k th bin and its number of elements. Let h_i be the normalized value, i.e., $h_i = \frac{H_k}{\sum_{i=1}^R H_i}$. We use the vector $\mathbf{F}_v = [h_1, \dots, h_R]$ to compute the activation pattern entropy E_j for the j th neuron. $E_j = -\sum_{i=1}^R h_i \cdot \log(h_i)$. The activation pattern entropy, E , of a deep learning model over all the neurons in all the fully connected layers is calculated as $E = \sum_{j=1}^N E_j$.

6 Dataset and Model Architecture

In our study, we used three benchmark datasets: MNIST [27], Fashion MNIST [47], CIFAR-10 [25] and one real-life dataset Plant village [30]. We also created MNIST Mixed and Fashion MNIST Mixed by randomizing the labels of the respective datasets to examine the reliability of the proposed metrics. The architecture for each dataset is illustrated in Table 1. The MNIST, Fashion MNIST, CIFAR-10 datasets each consists of 10 classes. There are 60,000 grayscale 28×28 images for training and 10,000 for testing in MNIST and Fashion MNIST, and 50,000 grayscale 32×28 images for training and 10,000 for testing in CIFAR-10.

The Plant village dataset consists of 28693 segmented color images of the healthy apple, blueberry and cherry, corn, grape, orange, peach and pepper, soybean, strawberry and squash, and tomato classes, and 6890 testing images. We transformed the color images to grayscale and reshaped the images to size 256×256 .

For all the models, apart from the input and output layers, we only used fully connected layers and dropout layer. For the fully connected layers, we used ReLU as the activation function, and Softmax activation for the output layer. For each model, we collected the weights and bias values from 20 iterations at a uniform interval. We denote the corresponding activation pattern graphs as $G(1), G(2), \dots, G(20)$. Since different models needed a different number of training iterations, this interval length varies, e.g., the CIFAR-10 model collected every two iterations, whereas the Plant Village model every five iterations. See the supplementary materials for detailed model architecture.

Table 1: Details of the architecture of the deep learning models for different datasets. In the model we only used fully connected (FC) and dropout layers.

Dataset	Image Size	Fully Connected Layers	Output Layer	Iterations	Training Accuracy (%)	Testing Accuracy (%)
MNIST	28×28	512, 512	10	20	99.56	98.24
MNIST Mixed	28×28	512, 512	10	20	12.44	9.85
Fashion MNIST	28×28	512, 512	10	20	91.80	88.9
Fashion MNIST Mixed	28×28	512, 512	10	20	11.02	10.12
CIFAR-10	32×32	1024, 1024, 1024, 512, 256, 128	10	40	46.24	43.43
Plant Village	256×256	8192, 2048, 1024, 512, 256, 128, 64	9	100	80.65	79.55

7 Result and Discussion

In this section, we describe the experimental results. To create the activation pattern graphs, we took 50 neurons per class (i.e., we choose $|S| = 50$ in Eq. 7) with the largest average activation value. We

Table 2: Two confusion matrices computed from layer 1 for MNIST dataset. Each matrix represents the number of unique neurons for pairwise classes. Darker red color represents a higher value.

		Iteration 1										Iteration 20									
20	1	9	8	7	14	11	7	7	4	30	0	7	5	3	6	7	4	5	2		
1	11	14	17	4	7	8	10	19	7	0	23	7	12	4	4	4	9	13	10		
9	14	13	17	5	9	16	4	15	5	7	7	11	13	8	3	13	7	16	8		
8	17	17	11	4	19	6	4	14	5	5	12	13	10	1	18	3	4	13	7		
7	4	5	4	11	11	11	14	14	28	3	4	8	1	19	5	10	10	12	24		
14	7	9	19	11	7	6	6	22	12	6	4	3	18	5	12	7	5	15	10		
11	8	16	6	11	6	16	5	7	3	7	4	13	3	10	7	18	3	10	8		
7	10	4	4	14	6	5	14	8	20	4	9	7	4	10	5	3	21	10	15		
7	19	15	14	14	22	7	8	3	20	5	13	16	13	12	15	10	10	5	21		
4	7	5	5	28	12	3	20	20	4	2	10	8	7	24	10	8	15	21	7		

repeated the experiments for the top 25 and top 100 neurons per class and achieved similar results.

7.1 Community Formation (H1)

Let $G(k)$ be a pattern activation graph of a fully connected layer at iteration k and let N_i be the set of neurons which are *representative* of the i th class, i.e., neurons that are frequently and highly activated for that class. The *unique* neurons of a pair of classes i and j are the neurons that belong to both N_i and N_j , but in no other set N_k where $k \notin \{i, j\}$. In other words, these neurons represents both classes i and j , but no other class. If $i = j$, then we obtain the unique neurons of class i . We observed that in most cases, the number of unique neurons for a single class increases with training, whereas unique neurons for a pair of distinct classes decrease. This behavior indicates that the overlap between the communities is decreasing and the classes are forming a stronger community among themselves. Table 2 compares the confusion matrices obtained from $G(1)$ and $G(20)$ for the MNIST dataset, where each entry at the diagonal of a matrix represents the unique neurons for a single class. We observed similar behavior for all the datasets.

Training Accuracy and Average Community Size: We used Gephi [1], a widely used graph visualization software, to compute force directed layouts [21] of the activation pattern graphs of different iterations. The communities were detected based on the Louvain method [3]. Although the visualization revealed community structures in these graphs, the change in the communities over the number of iterations was not readily visible from the graph layouts (see the supplementary material). Hence, we quantitatively examined how the number of nodes per community varies over the training. For each dataset, we used Gephi’s modularity function with a resolution value of 0.5 to find the communities in $G(1), G(2), \dots, G(20)$. Table 3 shows the number of nodes in the eight largest communities C_1, C_2, \dots, C_8 in layer 2 for different datasets and for two different iterations 1 and 20, where the distribution of community sizes appears to be less skewed over the training. We then perform the Pearson Correlation Coefficient (PCC) between the training accuracy and average node per community over the 10 iterations. For most of the datasets, we observed the average node per community to have a positive correlation with the training accuracy (Table 3), i.e., the PCC correlation was higher than 0. However, the weak (near-zero) correlation coefficient for MNIST Mixed and Fashion MNIST Mixed represents the randomness of the formation of the communities of the model. This indicates that, for models with good performance, the number of well defined communities increases with training and supports hypothesis **H1**.

7.2 Modularity and Accuracy (H2)

So far, we have observed that community detection can reveal meaningful clusters in the pattern activation graph, i.e., clusters are related to representative neuron sets for different classes. We now examine the other side, i.e., can the representative neuron sets for different classes be seen as well as the defined communities? To assess this, we compute different modularity metrics (Eq. 2– 4) for the activation pattern graphs $G(1), \dots, G(20)$. We also used different community detection algorithms available in the python library NetworkX [17] and iGraph [8]. Note that these algorithms take an initial partition of the neurons and then change those partitions to optimize some quality measure. Therefore, they are not suitable in this context, yet, the Kernighan Lin Bisection (KLB) [23] could generate consistent results.

We computed the Spearman correlation coefficient (SCC) and Pearson correlation coefficient (PCC) to examine the potential relation between modularity and training accuracy (Table 4). A positive correlation

Table 3: Number of nodes in different communities of the activation pattern graph (detected by Gephi). For each dataset, the communities of $G(1)$ and $G(20)$ are shown along with the PCC between the average node per community and training accuracy. Darker red color represents higher value.

MNIST									
Iteration	C1	C2	C3	C4	C5	C6	C7	C8	PCC
1	35	33	35	34	28	25	25	26	
20	38	37	36	36	34	33	31	30	0.52

Fashion MNIST Mixed									
Iteration	C1	C2	C3	C4	C5	C6	C7	C8	PCC
1	9	7	6	6	5	5	4	3	
20	10	7	7	7	7	6	5	5	0.28

MNIST Mixed									
Iteration	C1	C2	C3	C4	C5	C6	C7	C8	PCC
1	7	5	5	5	4	4	4	3	
20	13	12	8	7	7	5	5	4	-0.27

CIFAR-10									
Iteration	C1	C2	C3	C4	C5	C6	C7	C8	PCC
1	12	12	11	9	6	6	6	4	
20	39	27	26	25	14	11	10	10	0.80

Fashion MNIST									
Iteration	C1	C2	C3	C4	C5	C6	C7	C8	PCC
1	35	16	16	14	11	10	8	7	
20	32	27	25	21	15	15	12	11	0.71

Plant Village									
Iteration	C1	C2	C3	C4	C5	C6	C7	C8	PCC
1	40	26	26	21	6	4	3	3	
20	62	62	46	35	34	12	5	4	0.82

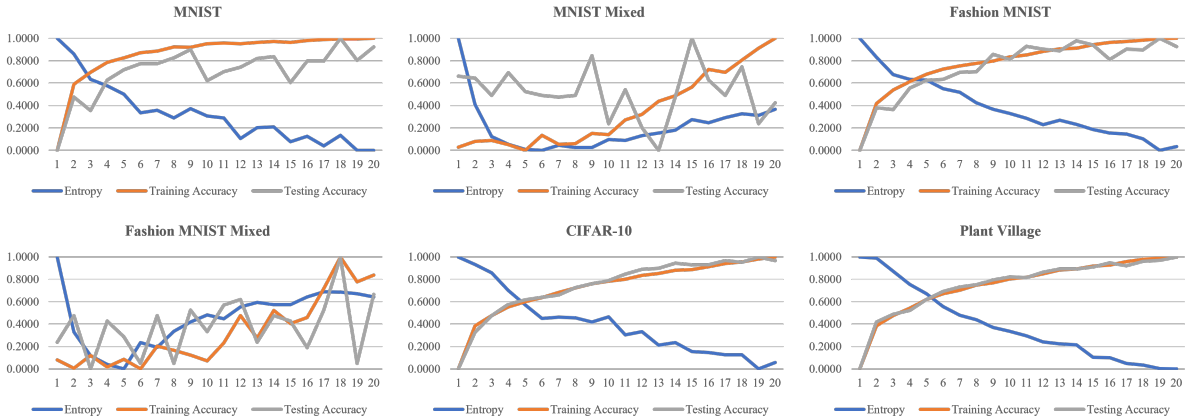


Figure 1: Change of normalized entropy, training and testing accuracy over different iterations.

value indicates that the communities’ quality is positively correlated with training accuracy. We observed the same relation with the test accuracy. A large number of strong positive correlation coefficients in Table 4 supports hypothesis **H2**. A stronger correlation is observed in later layers for all the dataset. For most datasets, the unweighted overlap (Eq. 3), and weighted overlap metric (Eq. 4) captures the relation better, which is expected since the no-overlap metric neither considers weight nor the community overlap.

7.3 Entropy and Accuracy (H3)

A higher entropy value represents more randomness in the activation behavior of a neuron. At the beginning of the training, due to random weights, the activation of the neuron is random. So, the entropy of the activation pattern over all the fully connected layers should be higher. As the training progresses, the entropy should decrease, representing a biased neuron activation behavior. Table 5 shows a negative correlation between the entropy of activation pattern and training accuracy over model training for most of the datasets. We observed the same relation with the test accuracy. Figure 1 shows the change of normalized entropy with training and testing accuracy for different iterations for all the datasets, where a clear relation between the entropy and model performance can be observed. However, MNIST Mixed and Fashion MNIST Mixed has positive correlation values, indicating the absence of activation pattern with training due to it’s random labels, which is consistent with hypothesis **H3**.

We also examine entropy change for individual classes, where to compute the entropy of a class, we take the same approach as in Section 5.2, but use only the training data corresponding to that class. In

Table 4: Spearman and Pearson correlation coefficient between modularity and training accuracy for different layers. Darker blue represents higher values and darker red represents lower values. (See the supplementary material for the relation with test accuracy.)

	MNIST				MNIST Mixed				Fashion MNIST				Fashion MNIST Mixed			
	L1		L2		L1		L2		L1		L2		L1		L2	
	PCC	SCC	PCC	SCC	PCC	SCC	PCC	SCC	PCC	SCC	PCC	SCC	PCC	SCC	PCC	SCC
KLB	0.24	0.16	0.50	0.61	-0.76	-0.81	-0.73	-0.84	-0.04	-0.10	0.42	0.44	-0.03	-0.07	-0.44	-0.38
No-overlap	0.22	0.19	0.23	0.19	-0.44	-0.55	0.46	0.37	0.42	0.46	0.62	0.61	0.28	0.40	0.14	0.29
Unweighted, Overlap	0.53	0.37	0.78	0.68	-0.70	-0.73	0.36	0.37	0.71	0.67	0.77	0.72	0.43	0.51	0.22	0.35
Weighted, Overlap	0.36	0.33	0.77	0.57	-0.63	-0.69	0.48	0.47	0.56	0.46	0.78	0.79	0.43	0.51	0.26	0.38
CIFAR-10																
	L1		L2		L3		L4		L5		L6					
	PCC	SCC	PCC	SCC	PCC	SCC	PCC	SCC	PCC	SCC	PCC	SCC	PCC	SCC	PCC	SCC
	KLB	0.16	0.20	0.68	0.74	0.69	0.73	-0.18	-0.13	-0.29	-0.40	-0.01	0.06			
No-overlap	-0.05	-0.11	0.62	0.66	0.29	0.27	0.06	-0.05	0.01	0.03	-0.49	-0.44				
Unweighted, Overlap	0.34	0.44	0.87	0.86	0.73	0.82	0.82	0.79	0.66	0.77	-0.37	-0.29				
Weighted, Overlap	0.42	0.55	0.78	0.68	0.71	0.78	0.71	0.70	0.71	0.79	0.02	-0.03				
Plant Village																
	L1		L2		L3		L4		L5		L6		L7			
	PCC	SCC	PCC	SCC	PCC	SCC	PCC	SCC	PCC	SCC	PCC	SCC	PCC	SCC	PCC	SCC
	KLB	0.22	0.16	0.57	0.62	0.76	0.61	0.84	0.83	-0.16	0.02	-0.34	-0.30	-0.21	-0.19	
No-overlap	0.24	0.15	0.05	0.03	0.40	0.42	-0.15	-0.10	0.04	0.00	0.03	-0.17	0.46	0.58		
Unweighted, Overlap	0.14	0.09	0.49	0.47	0.83	0.80	0.91	0.85	0.63	0.65	0.46	0.47	0.74	0.82		
Weighted, Overlap	0.24	0.26	0.59	0.52	0.84	0.87	0.88	0.78	0.71	0.78	0.66	0.69	0.62	0.72		

Table 5: Spearman and Pearson correlation coefficient between the entropy and training accuracy. Darker blue represents higher values and darker red represents lower values.

	MNIST	MNIST Mixed	Fashion MNIST	Fashion MNIST Mixed	CIFAR-10	Plant Village
PCC	-0.87	0.22	-0.95	0.57	-0.95	-0.94
SCC	-0.94	0.51	-0.99	0.67	-0.97	-1

Table 6: Spearman and Pearson correlation coefficient between entropy and training accuracy for individual classes. Darker blue represents higher values, and darker red represents lower values.

Class	MNIST		MNIST Mixed		Fashion MNIST		Fashion MNIST Mixed		CIFAR-10		Plant Village	
	PCC	SCC	PCC	SCC	PCC	SCC	PCC	SCC	PCC	SCC	PCC	SCC
1	-0.55	-0.67	-0.06	-0.29	0.1	0.21	-0.13	-0.4	0.22	0.17	-0.85	-0.89
2	-0.54	-0.71	0.18	-0.16	-0.24	-0.45	0.77	-0.15	0.7	0.66	-0.86	-0.93
3	-0.22	-0.31	0.47	-0.02	0.37	0.22	0.47	0.31	0.38	-0.1	-0.46	-0.42
4	-0.35	-0.7	0.36	0.11	-0.57	-0.84	0.25	-0.18	0.13	0.16	-0.88	-0.92
5	-0.71	-0.73	0.33	-0.1	-0.41	-0.30	0.48	0.11	-0.40	-0.53	-0.39	-0.25
6	-0.55	-0.52	-0.14	-0.07	-0.67	-0.67	0.33	-0.17	-0.5	-0.51	-0.86	-0.86
7	0	0.16	0.19	0.44	-0.83	-0.95	0.67	0.17	0.59	-0.17	-0.87	-0.89
8	-0.09	-0.29	0.09	0.33	-0.43	-0.62	0.7	0.3	0.16	0.19	-0.91	-0.89
9	-0.67	-0.8	0.46	0.62	-0.9	-0.96	0.63	0.33	0.01	0.14	-0.81	-0.86
10	-0.39	-0.77	0.09	0.01	-0.67	-0.60	0.90	0.86	-0.18	-0.26	-	-

this setting, we obtain meaningful results (i.e., a negative correlation between the entropy and training accuracy) only for all well-trained models (MNIST, Fashion MNIST, and Plant Village). However, there are few classes with positive and small negative correlation between entropy and accuracy. This is due to frequent change in the training accuracy of that class. For CIFAR-10, MNIST Mixed, Fashion MNIST Mixed, we observed a positive correlation values in most of the classes, and sometimes even found the correlation coefficient to be strongly positive. This is due to the inability of the model to separate the classes from one another.

8 Limitations and Future Work

We have proposed novel methods to explain the behavior of neurons in deep learning models as the model training progresses. We used graph theoretic and entropy-based methods to model the activation pattern of the neurons. We quantitatively showed that neurons that are highly activated for a class form a community in our graph model. For the entropy-based approach, we analyzed the activation pattern using the Shannon entropy and found the entropy to show a negative correlation with the training accuracy.

There are many scope for future research. We used deep learning models with only fully connected layers; using different model architecture may help understand the entropy and modularity behavior with more granularity. Although we examine a diverse set of datasets, adding more datasets could strengthen the results. Our experimental results show that the modularity of the activation pattern graph and entropy of the activation pattern is related to the model's performance. Although we used widely used quality measures for the modularity and entropy, there is still scope for designing better quality metrics specifically for neural network context.

Our study lays the initial groundwork for graph and entropy-based studies to analyze the deep learning models' performance. We believe that our results will inspire further research to explain the deep learning models using graph and information theoretic methods.

Acknowledgement

This work is supported by the Natural Sciences and Engineering Research Council of Canada (NSERC), and by two Canada First Research Excellence Fund (CFREF) grants coordinated by Global Institute for Food Security (GIFS) and Global Institute for Water Security (GIWS).

References

- [1] M. Bastian, S. Heymann, and M. Jacomy. Gephi: an open source software for exploring and manipulating networks. In *Proceedings of the International AAAI Conference on Web and Social Media*, volume 3, 2009.
- [2] D. Bau, B. Zhou, A. Khosla, A. Oliva, and A. Torralba. Network dissection: Quantifying interpretability of deep visual representations. In *Proceedings of the IEEE conference on computer vision and pattern recognition*, pages 6541–6549, 2017.
- [3] V. D. Blondel, J.-L. Guillaume, R. Lambiotte, and E. Lefebvre. Fast unfolding of communities in large networks. *Journal of statistical mechanics: theory and experiment*, 2008(10):P10008, 2008.
- [4] M. Borowska. Entropy-based algorithms in the analysis of biomedical signals. *Studies in Logic, Grammar and Rhetoric*, 43(1):21–32, 2015.
- [5] D. Chen, M. Shang, Z. Lv, and Y. Fu. Detecting overlapping communities of weighted networks via a local algorithm. *Physica A: Statistical Mechanics and its Applications*, 389(19):4177–4187, 2010.
- [6] S. Chung, S. Suh, C. Park, K. Kang, J. Choo, and B. C. Kwon. Revacnn: Real-Time visual analytics for convolutional neural network. 2016.
- [7] A. Clauset, M. E. Newman, and C. Moore. Finding community structure in very large networks. *Physical review E*, 70(6):066111, 2004.

- [8] G. Csardi and T. Nepusz. The igraph software package for complex network research. *InterJournal, Complex Systems*:1695, 2006.
- [9] A. Dobrescu, M. Valerio Giuffrida, and S. A. Tsafaris. Understanding deep neural networks for regression in leaf counting. In *Proceedings of the IEEE/CVF Conference on Computer Vision and Pattern Recognition Workshops*, pages 0–0, 2019.
- [10] J. Duch and A. Arenas. Community detection in complex networks using extremal optimization. *Physical review E*, 72(2):027104, 2005.
- [11] R. Fong and A. Vedaldi. Net2vec: Quantifying and explaining how concepts are encoded by filters in deep neural networks. In *Proceedings of the IEEE conference on computer vision and pattern recognition*, pages 8730–8738, 2018.
- [12] S. Fortunato and C. Castellano. Community structure in graphs. *arXiv preprint arXiv:0712.2716*, 2007.
- [13] A. Gaier and D. Ha. Weight agnostic neural networks. *arXiv preprint arXiv:1906.04358*, 2019.
- [14] A. Géron. *Hands-on machine learning with Scikit-Learn, Keras, and TensorFlow: Concepts, tools, and techniques to build intelligent systems*. O’Reilly Media, 2019.
- [15] S. Gigante, A. S. Charles, S. Krishnaswamy, and G. Mishne. Visualizing the phate of neural networks. In *NeurIPS*, 2019.
- [16] R. M. Gray. *Entropy and information theory*. Springer Science & Business Media, 2011.
- [17] A. Hagberg, P. Swart, and D. S Chult. Exploring network structure, dynamics, and function using networkx. Technical report, Los Alamos National Lab.(LANL), Los Alamos, NM (United States), 2008.
- [18] A. W. Harley. An interactive node-link visualization of convolutional neural networks. In *International Symposium on Visual Computing*, pages 867–877. Springer, 2015.
- [19] F. Hohman, M. Kahng, R. Pienta, and D. H. Chau. Visual analytics in deep learning: An interrogative survey for the next frontiers. *IEEE transactions on visualization and computer graphics*, 25(8):2674–2693, 2018.
- [20] F. Hohman, H. Park, C. Robinson, and D. H. P. Chau. S ummit: Scaling deep learning interpretability by visualizing activation and attribution summarizations. *IEEE transactions on visualization and computer graphics*, 26(1):1096–1106, 2019.
- [21] M. Jacomy, T. Venturini, S. Heymann, and M. Bastian. Forceatlas2, a continuous graph layout algorithm for handy network visualization designed for the gephi software. *PloS one*, 9(6):e98679, 2014.
- [22] M. Kahng, P. Y. Andrews, A. Kalro, and D. H. Chau. Activis: Visual exploration of industry-scale deep neural network models. *IEEE transactions on visualization and computer graphics*, 24(1):88–97, 2017.
- [23] B. W. Kernighan and S. Lin. An efficient heuristic procedure for partitioning graphs. *The Bell system technical journal*, 49(2):291–307, 1970.
- [24] B. Kim, M. Wattenberg, J. Gilmer, C. Cai, J. Wexler, F. Viegas, et al. Interpretability beyond feature attribution: Quantitative testing with concept activation vectors (tcav). In *International conference on machine learning*, pages 2668–2677. PMLR, 2018.
- [25] A. Krizhevsky, V. Nair, and G. Hinton. Cifar-10 (canadian institute for advanced research). 2009.
- [26] Y. LeCun, Y. Bengio, and G. Hinton. Deep learning. *Nature*, 521(7553):436–444, 2015.
- [27] Y. LeCun, C. Cortes, and C. Burges. Mnist handwritten digit database. *ATT Labs [Online]*. Available: <http://yann.lecun.com/exdb/mnist>, 2, 2010.

- [28] H. Li, Z. Xu, G. Taylor, C. Studer, and T. Goldstein. Visualizing the loss landscape of neural nets. *arXiv preprint arXiv:1712.09913*, 2017.
- [29] A. Mahendran and A. Vedaldi. Understanding deep image representations by inverting them. In *Proceedings of the IEEE conference on computer vision and pattern recognition*, pages 5188–5196, 2015.
- [30] S. P. Mohanty. Plant village. <https://github.com/spMohanty/PlantVillage-Dataset>, 2018.
- [31] M. E. Newman. Fast algorithm for detecting community structure in networks. *Physical review E*, 69(6):066133, 2004.
- [32] M. E. Newman and M. Girvan. Finding and evaluating community structure in networks. *Physical review E*, 69(2):026113, 2004.
- [33] V. Nicosia, G. Mangioni, V. Carchiolo, and M. Malgeri. Extending the definition of modularity to directed graphs with overlapping communities. *Journal of Statistical Mechanics: Theory and Experiment*, 2009(03):P03024, 2009.
- [34] S. J. Oh, B. Schiele, and M. Fritz. Towards reverse-engineering black-box neural networks. In *Explainable AI: Interpreting, Explaining and Visualizing Deep Learning*, pages 121–144. Springer, 2019.
- [35] C. Olah, A. Mordvintsev, and L. Schubert. Feature visualization. *Distill*, 2(11):e7, 2017.
- [36] A. Rai. Explainable ai: From black box to glass box. *Journal of the Academy of Marketing Science*, 48(1):137–141, 2020.
- [37] C. Rudin. Stop explaining black box machine learning models for high stakes decisions and use interpretable models instead. *Nature Machine Intelligence*, 1(5):206–215, 2019.
- [38] B. Shahriari, K. Swersky, Z. Wang, R. P. Adams, and N. De Freitas. Taking the human out of the loop: A review of bayesian optimization. *Proceedings of the IEEE*, 104(1):148–175, 2015.
- [39] C. E. Shannon. A mathematical theory of communication. *ACM SIGMOBILE mobile computing and communications review*, 5(1):3–55, 2001.
- [40] H. Shen, X. Cheng, K. Cai, and M.-B. Hu. Detect overlapping and hierarchical community structure in networks. *Physica A: Statistical Mechanics and its Applications*, 388(8):1706–1712, 2009.
- [41] E. H. Shortliffe and B. G. Buchanan. A model of inexact reasoning in medicine. *Mathematical biosciences*, 23(3-4):351–379, 1975.
- [42] M. Simon, E. Rodner, and J. Denzler. Part detector discovery in deep convolutional neural networks. In *Asian Conference on Computer Vision*, pages 162–177. Springer, 2014.
- [43] K. Simonyan, A. Vedaldi, and A. Zisserman. Deep inside convolutional networks: Visualising image classification models and saliency maps. *arXiv preprint arXiv:1312.6034*, 2013.
- [44] D. Smilkov, S. Carter, D. Sculley, F. B. Viégas, and M. Wattenberg. Direct-manipulation visualization of deep networks. *arXiv preprint arXiv:1708.03788*, 2017.
- [45] F.-Y. Tzeng and K.-L. Ma. *Opening the black box-data driven visualization of neural networks*. IEEE, 2005.
- [46] K. Wongsuphasawat, D. Smilkov, J. Wexler, J. Wilson, D. Mane, D. Fritz, D. Krishnan, F. B. Viégas, and M. Wattenberg. Visualizing dataflow graphs of deep learning models in tensorflow. *IEEE transactions on visualization and computer graphics*, 24(1):1–12, 2017.
- [47] H. Xiao, K. Rasul, and R. Vollgraf. Fashion-mnist: a novel image dataset for benchmarking machine learning algorithms. *arXiv preprint arXiv:1708.07747*, 2017.

- [48] M. D. Zeiler and R. Fergus. Visualizing and understanding convolutional networks. In *European conference on computer vision*, pages 818–833. Springer, 2014.
- [49] H. Zeng, H. Haleem, X. Plantaz, N. Cao, and H. Qu. Cnncomparator: Comparative analytics of convolutional neural networks. *arXiv preprint arXiv:1710.05285*, 2017.
- [50] Q. Zhang, R. Cao, F. Shi, Y. N. Wu, and S.-C. Zhu. Interpreting cnn knowledge via an explanatory graph. In *Proceedings of the AAAI Conference on Artificial Intelligence*, volume 32, 2018.
- [51] B. Zhou, A. Khosla, A. Lapedriza, A. Oliva, and A. Torralba. Object detectors emerge in deep scene cnns. *arXiv preprint arXiv:1412.6856*, 2014.